How to cite: *Angew. Chem. Int. Ed.* **2022,** *61,* e202211138
International Edition: doi.org/10.1002/anie.202211138
German Edition: doi.org/10.1002/ange.202211138

VIP **Foldamers** **Very Important Paper**

Differential Peptide Multi-Macrocyclizations at the Surface of a Helical Foldamer Template

*Sebastian Dengler, Céline Douat, and Ivan Huc**

Abstract: Hybrid sequences comprising a peptide with several Cys residues and an aromatic foldamer helix with several chloroacetamide functions at its surface were synthesized. Such products may in principle form numerous macromulticyclic thioether products by intramolecularly combining all Cys residues and all chloroacetamide functions. However, we show that the reactive sites on the structurally defined helix can be placed at such locations that the peptide selectively stitches itself to form a series of different macrocycles within mostly one preferred product. Reactions were monitored by HPLC and products with two, three or four macrocycles were identified using LC–MS and NMR. The series of selective macrocyclizations define a sort of reaction trail where reaction sites otherwise identical are involved successively because of their precise positioning in space. The trails can be predicted to a large extent based on structural considerations and the assumption that smaller macrocycles form faster.

Introduction

The importance of cyclic and macrocyclic molecules in chemistry cannot be overstated. It generally stems from the benefits provided by their limited conformational freedom. Innumerable cyclization methods have been reported and the key role played by stereochemical and conformational preorganization in these reactions has been thoroughly highlighted.[1,2] Macrocyclic peptides are a large subclass of cyclic molecules with a high potential to bind protein target surfaces.[3] Multiple peptide macrocyclization reactions have been validated[4,5] some of which, e.g. the simple substitution of a chloromethylene function by the thiol of a Cys residue to form a thioether, are so efficient that they can be performed reliably and concomitantly on libraries of trillions of different peptides for display selection.[3,6]

At the exclusion of ladder polymers where the same cyclization step is repeated many times,[7] preparing molecules with multiple cycles generally requires elaborate strategies. The careful positioning of reactive functions on a small molecule may lead to a reaction cascade that produces several different rings at once.[8] Bimacrocycles of variable size and composition can be efficiently produced from peptides containing three Cys residues and a 1,3,5-tris-bromomethyl platform, thanks to the C_3-symmetry of the platform which yields the same product regardless of which Cys residue reacts first, second or third.[9] Typical synthetic and biosynthetic strategies to produce multimacrocyclic molecules rely on independent cyclization steps involving different reaction groups, which can be cumbersome. Yet some notable exceptions exist. For example, chemical and stereochemical preferences in disulfide bridge formation, including the fact that disulfides are subject to exchange reactions, have allowed for the direct preparation of complex multicycles.[9b,10] In proteins as well, specific arrays of disulfide bridges may form, directed by both structural control (folding) and disulfide exchange (mediated by protein disulfide isomerases).[11]

Here, we report that a series of different peptide macrocycles may form selectively at the surface of a structurally well-defined aromatic oligoamide foldamer helix derived from δ-amino acids. In contrast with the above examples of multimacrocyclization, the functionalities involved are all identical—up to four thiols and four chloroacetamides—and reactions are irreversible. Selective macrocyclizations take place at the expense of the multiple intramolecular products that may in principle be expected. Selectivity is predictable and appears to be guided by ring size, with the smallest ring forming first, reducing the size of the subsequent smallest ring, and by the structural organization imparted by the aromatic helix which places some reactive centers out of the reach of others. The outcome is a sort of reaction trail[12] along which a flexible peptide chain stitches itself in a certain order to bridge reactive centers at the surface of a well-defined molecular scaffold. The products consist of a compact hydrophobic core (the aromatic helix) surrounded by peptide loops. They are reminiscent of protein structures and might thus find use as multivalent protein binders.

[*] S. Dengler, Dr. C. Douat, Prof. Dr. I. Huc
Department of Pharmacy and Center for Integrated Protein Science, Ludwig-Maximilians-Universität
Butenandtstr. 5–13, 81377 München (Germany)
E-mail: ivan.huc@cup.lmu.de

Results and Discussion

Design and synthesis

We have previously reported the formation of helical aromatic oligoamide foldamer/peptide hybrid macrocycles via the substitution of an N-terminal chloroacetamide on the foldamer helix by a Cys thiol near the C-terminus of the peptide (Figure 1, left).[13] Interest for these compounds followed the discovery that they may be produced—when the foldamer is short enough—by ribosomal peptide translation through reprogramming the initiation step with a foldamer-functionalized tRNA, paving the way to display selection experiments.[14] Aromatic foldamers containing 4-substituted 8-amino-2-quinoline carboxylic acid units (Q^{Xxx}, Figure 2a) adopt particularly stable helical conformations in water.[15] Within the macrocycles, the folding propensity of the aromatic segments was shown to influence peptide conformation and enhance peptide resistance toward proteolytic degradation and, in a reciprocal effect, the chirality of the peptides was shown to bias foldamer helix handedness.[13,14]

Encouraged by this background, we set out to test whether a large peptide loop may be connected more than once to the rigid foldamer helix, *de facto* further reducing its conformational freedom and creating several different macrocycles (Figure 1). For this purpose, we prepared a series of foldamer-peptide hybrids in which the peptide contains a variable number of Cys residues separated by loops of different sizes, and the foldamer displays chloroacetamides as side chain appendages at different positions of the helix, and investigated their cyclization. Systematic variations of the peptide sequences were not considered for this study. Nevertheless, the peptides were designed so as to contain diverse sequences, keeping some polar residues to preserve water solubility and avoiding synthetically demanding residues (e.g. Pro, Val, His). A generic structure is shown in Figure 2b. To simplify the presentation, the foldamer units are numbered from the C-terminus while the α-amino acid residues (AAs) are numbered from the N-terminus. Thus, all sequences comprise a $Q^{Asp}1$-Gly1 linkage at the foldamer-peptide junction. All sequences also comprise a $B^{Rme}4$ unit near the middle of the foldamer segment. This chiral residue quantitatively biases helix handedness towards its left-handed conformation.[16] Typically, induced CD bands indicate handedness bias and a single set of signals on ^{1}H NMR spectra as well as a single HPLC peak confirm full handedness control.[13] The foldamer segment generally consisted of Q^{Asp} and Q^{Dap} charged residues to provide solubility in both basic and acidic aqueous media and was acetylated or acylated with a short diethyleneglycol-containing acid at the N-terminus. A new Alloc-protected Fmoc-$Q^{Dap(Alloc)}$-OH monomer was synthesized to anchor chloroacetamide functions at the final stage of solid phase synthesis.

Synthetic methods and protocols are described in detail in the Supporting Information. Typically, the Cys-containing peptide was first prepared via conventional Fmoc-based chemistry under microwave irradiation and phosphonium-based coupling conditions (i.e. PyBOP and DIPEA) on a low loading Fmoc-Gly-Wang resin (scale 50–100 μmol). From there, solid phase foldamer synthesis can be continued with Fmoc-Q^{Xxx} monomers, including some $Q^{Dap(Alloc)}$, and Appel coupling conditions.[15a,17] We also validated the

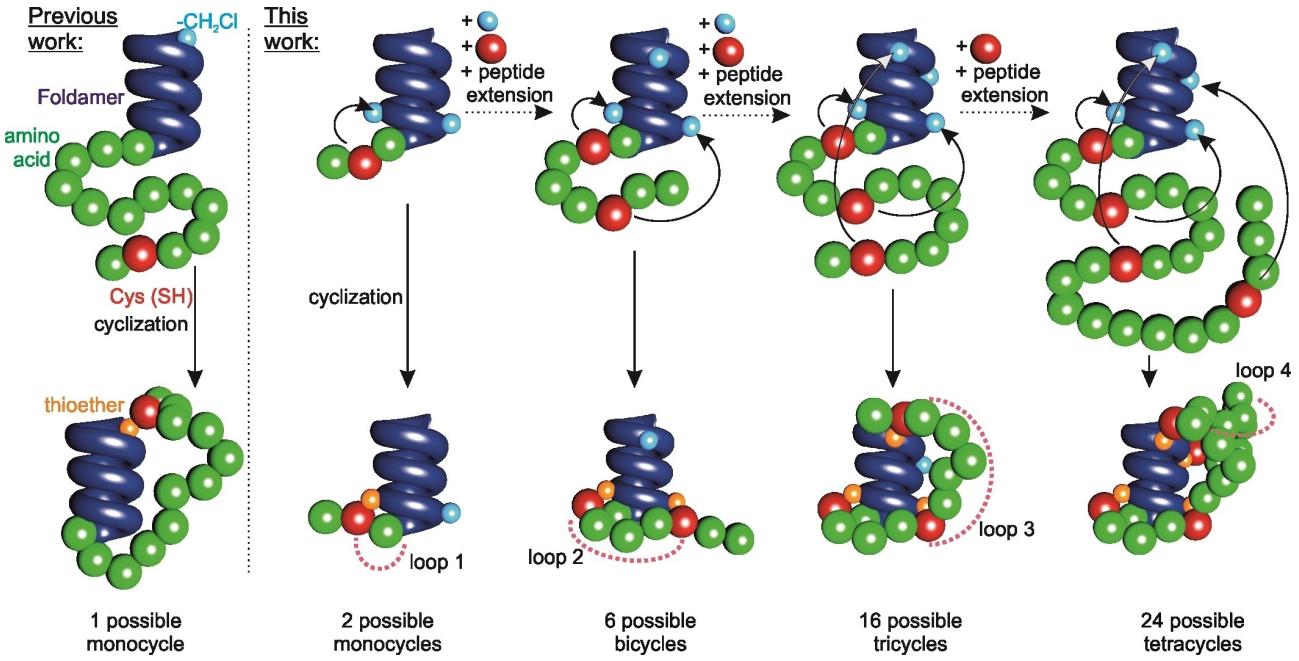

Figure 1. Schematic illustration of selective macrocyclizations of helical aromatic foldamer-peptide hybrids. The foldamer is shown as a blue helix tube and the peptide as a string of balls. Upon careful positioning of chloroacetamide electrophiles on the helix and of Cys thiols in the peptide sequence, i.e. through the adjustment of peptide loop size, selective reaction trails[12] can be programmed to form multicyclic products.

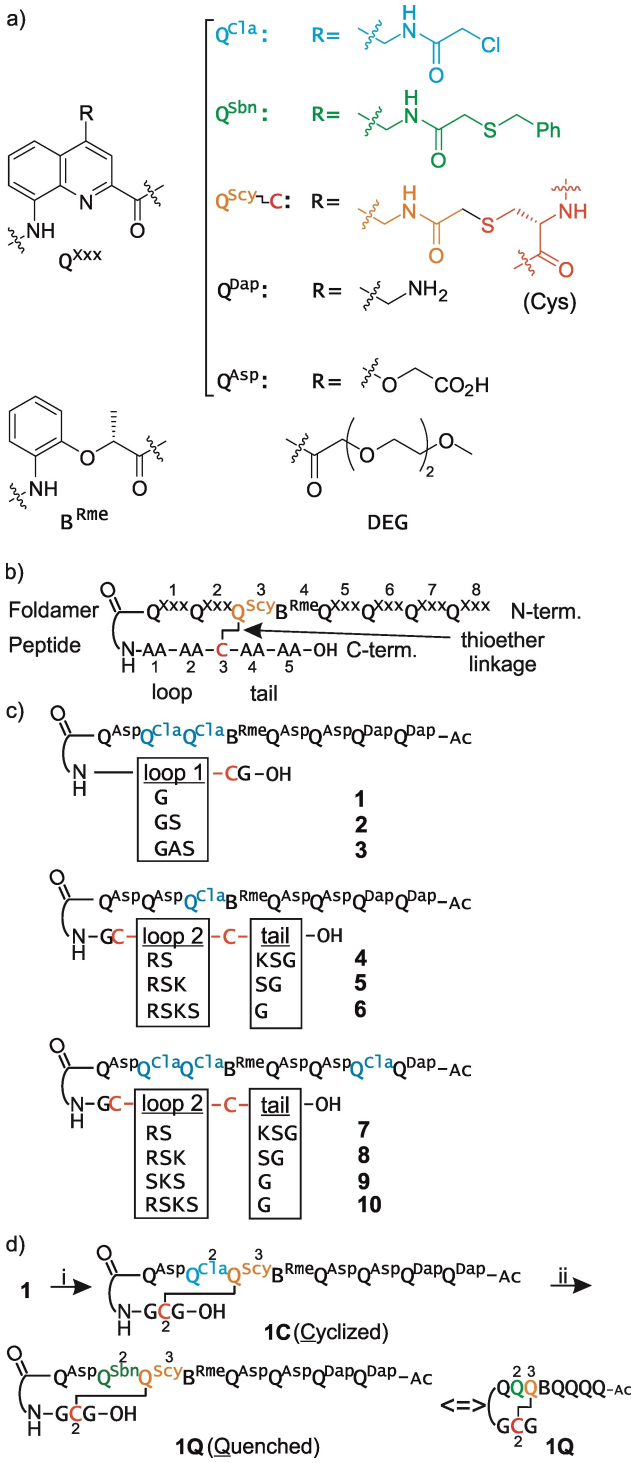

Figure 2. a) Foldamer building blocks. b) Generic cyclic foldamer-peptide hybrid defining sequence numbering, peptide loops, and tail. c) Sequences with variable loop sizes investigated for the preparation of mono and bicyclic structures. Amino acids are designated by the single letter code. d) Representative reaction scheme from **1** towards monocycle **1C** and its quenched derivative **1Q**. (*i*) aqueous basic conditions; (*ii*) addition of benzyl mercaptan. A simplified depiction of **1Q** is also shown and used in other figures. Note that Q within the foldamer segment refers to a color-coded Q^{Xxx} quinoline-based monomer (as in (a)), not to glutamine (Q, Gln) which may also be present in the peptide or the letter Q used in the quenched products (e.g. **1Q**).

possibility to presynthesize and purify a protected Fmoc-foldamer-Gly-OH segment on SASRIN® resin and ligate it directly to the resin-bound free amine peptide (see ESI section 2.4.3.3.). With the protected foldamer-peptide hybrid still on the resin, Alloc protections were selectively removed and the corresponding Q^{Dap} monomers were converted into Q^{Cla} units (Figure 2a) with chloroacetic anhydride. After TFA cleavage and side chain deprotection, the purification of the hybrid oligomers was carried out by semi-preparative RP-HPLC in acidic media (hence the importance of solubility). At pH 2, the thiols and chloroacetamides did not react. The linear foldamer-peptide hybrids were recovered in good to moderate yields with purity over 95 %.

Cyclizations were triggered under basic conditions (TEA buffer pH 10 or $NaHCO_3$ buffer pH 8.5),[18] converting Q^{Cla} units into Q^{Scy} connected to a Cys residue by a thioether. Low concentrations (25–100 μM) favored intramolecular processes. Oxygen was removed in most cases by freeze-pump-thaw cycles and tris(2-carboxyethyl)phosphine (TCEP) was further added to avoid disulfide formation. Acetonitrile was added to enhance solubility. Urea (8 M) was sometimes used as a chaotropic additive (see below). Progression of the cyclizations could be monitored by RP-HPLC and mass spectrometry (LC-ESI-MS, see Figures S2, S4–S17, S20–S26, S29–S31). Conversion yields were estimated by integrating HPLC peak areas against an internal reference. After cyclization, unreacted chloroacetamides could be quenched with benzyl mercaptan yielding hydrophobic Q^{Sbn} units. Fmoc-Q^{Sbn}-OH was also synthesized and incorporated directly in some sequences to ascertain compound identification (Figures S3, S18, S19, S27, S28). Sequences **4**–**6** which possess an excess number of Cys residues were also quenched using a chloroacetamide solution (Figures S6–8).

Monocycle formation

Examination of molecular models showed that the side chain in position 4 of Q3 was the closest to the N-terminal residues of the peptide and might react first if the smallest ring size is favored during macrocyclization. The side chain of Q2 and possibly Q1, Q5, and Q7 would be the next nearest sites. More remote positions were expected to be out of reach of AAs close to the N-terminus. Thus, sequences **1**–**3** were designed to test the selectivity of macrocyclization between a Cys residue in positions 2, 3 or 4 and chloroacetamides on $Q^{Cla}2$ and $Q^{Cla}3$. Cyclization was complete after only five minutes. While **2** and **3** generated two products (**2C-a** and **2C-b**, and **3C-a** and **3C-b**, respectively), **1** yielded a single product **1C** (Figures 2d, 3a–c). Separation of the peaks and MS analysis confirmed that all compounds corresponded to a cyclic adduct. The unreacted chloroacetamide functions were quenched with benzyl mercaptan. The products (**1Q**, **2Q-a/b**, **3Q-a/b**) were all separated and identified by LC-ESI-MS analysis. Thus, selective cyclization occurs only with **1** which has the shortest loop1, consisting of a single Gly residue. Proof that Cys2 has cyclized with $Q^{Cla}3$ in **1C** and **1Q** was obtained by

independently synthesizing a reference sequence (**R1**) using $Q^{Cla}3$ and $Q^{Sbn}2$ instead of $Q^{Cla}3$ and $Q^{Cla}2$. After cyclization, ^{1}H NMR and HPLC analyses confirmed **R1** to be identical to **1Q** (Figures 3d, S3). This shortest loop1 was kept in all subsequent designs.

A second series of sequences was then prepared containing $Q^{Cla}3$ and Cys2, and also a second Cys residue in positions 5, 6 or 7 (**4**–**6** in Figure 2c). Cyclization was again quick. A single product was observed with **5** and **6**, and two with **4** (Figure 3a-c). In these early experiments, TCEP had not been added initially. As a consequence, intramolecular cyclization was followed by intermolecular disulfide bridge formation, as confirmed by LC–MS analysis. Subsequent addition of TCEP reduced the disulfides and all products showed a mass consistent with one thioether and one free thiol function. The latter could be quenched with excess chloroacetamide. We inferred that the Cys2/$Q^{Cla}3$ reaction remains clean even in the presence of a second Cys residue provided that the latter is at least three amino acids apart (as in **5** and **6**). Compound **4** has a shorter loop2 and Cys5 apparently competes with Cys2.

Bicycle formation

Careful examination of molecular models then suggested that a Cys residue in position 6 or 7 left free after the Cys2/$Q^{Cla}3$ reaction might reach a chloroacetamide on Q2, with Q7 being just a little more remote and other Q units being further away. The rationale was again that the smallest ring would form the fastest. Compounds **7**–**10** were then prepared, all having $Q^{Cla}2$, $Q^{Cla}3$ and $Q^{Cla}7$ reactive centers, and two Cys residues, one in position 2 and the other in position 5, 6 or 7, as in **4**–**6**. The cyclization of **7**, with the smallest loop2, was nonselective, consistent with the behavior of **4** (Figure 3a,b). The major product **7C-a** has the mass expected for a bicycle, yet a monocyclic product (**7C-b**) was also detected. The monocycle was interpreted as resulting from a Cys5/$Q^{Cla}3$ reaction, that leaves Cys2 unable to reach $Q^{Cla}2$ or $Q^{Cla}7$.

The cyclization of **8**, **9** and **10** progressed selectively towards a bicycle, as identified by LC–MS (Figure 3a–c). The remaining, unreacted chloroacetamide function was then quenched with benzyl mercaptan to yield **8Q**, **9Q** and **10Q** which were all isolated in pure form by RP-HPLC (Figures S10–12). Based on the models, the bicyclization pattern of **8**–**10**, as well as the major bicyclization product of **7**, were thought to result from a Cys2/$Q^{Cla}3$ reaction followed by a CysX/$Q^{Cla}2$ with X = 5–7, leaving $Q^{Cla}7$ free to react with benzyl mercaptan. This reaction trail leads to a sort of crossing of the thioether bridges (Figure 3c, left).

The reaction trail was ascertained by the NMR structural assignment of **9Q** (Supporting Information section 1.2). Key for the assignment were NOESY correlations involving the amide NH of the side chain in Q^{Sbn} and Q^{Scy} units. Thus, a correlation between the side chain NH of $Q^{Scy}3$ and the Cys2 NH, and a correlation between the side chain NH of $Q^{Scy}2$ and the Cys7 NH were observed. Consistently, the side chain NH of $Q^{Sbn}7$ correlated with the benzylic CH_2. NMR assignment also revealed characteristic signals suggesting that the peptide has a defined conformation (Figure S43).

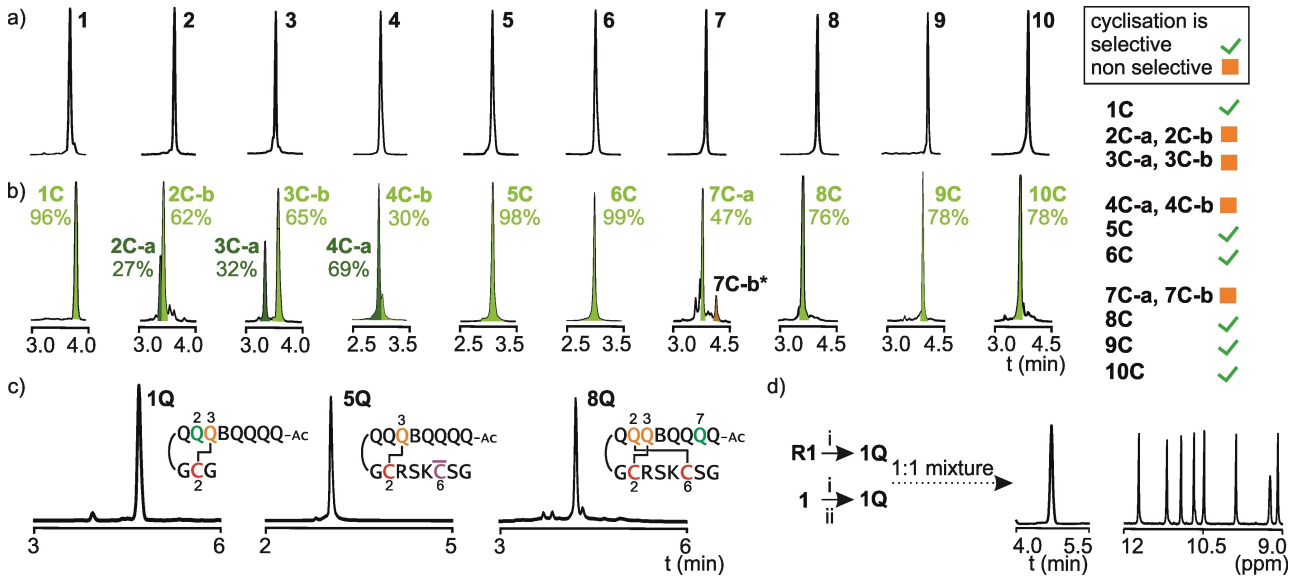

Figure 3. HPLC chromatograms of compounds **1**–**10** before (a) and after cyclization (b). Percentages indicate yields calculated by peak integration and comparison with an internal standard. c) HPLC chromatograms and schematic formula of quenched products **1Q**, **5Q** and **8Q**. Q^{Xxx} units are color-coded as in Figure 2a. Green indicates a benzyl thioether side chain (Q^{Sbn}). Purple $\bar{C}$ indicates Cys(CH_2CONH_2) from the quenching of Cys residue with chloroacetamide. d) HPLC chromatogram and excerpt of the ^{1}H NMR spectrum (aromatic NH resonances) of a 1:1mixture of **1Q** produced by quenching of **1C**, and **1Q** produced by cyclization of **R1**.

Tricycle formation

In summary of the above, **8**–**10** may form two macrocycles with high selectivity leaving $Q^{Cla}7$ free for a subsequent reaction. Triple cyclization was therefore attempted by adding one Cys residue further in the peptide sequence. Sequences **11**–**14** were then designed (Figure 4a). They all comprise the same loop1 (-Gly-) and loop2 (-Ser-Lys-Ser-) expected to promote Cys2/$Q^{Cla}3$ and Cys6/$Q^{Cla}2$ reactions, and a third loop of variable size before a cysteine in position 9, 10, 11 or 12. This Cys residue was expected to react with $Q^{Cla}7$. Anticipating the next increment, **11**–**14** also comprise a fourth chloroacetamide electrophile on $Q^{Cla}6$. This unit is located on the other side of the helix and in principle out of reach of cysteines in position 8 to 11, at the condition the peptide is already stitched to the foldamer by Cys2 and Cys6, i.e. that the smallest macrocycles have formed first. Compounds **11**–**14** contain seven aromatic units instead of eight for **1**–**10** because Q8 was considered to be unneeded at this stage.

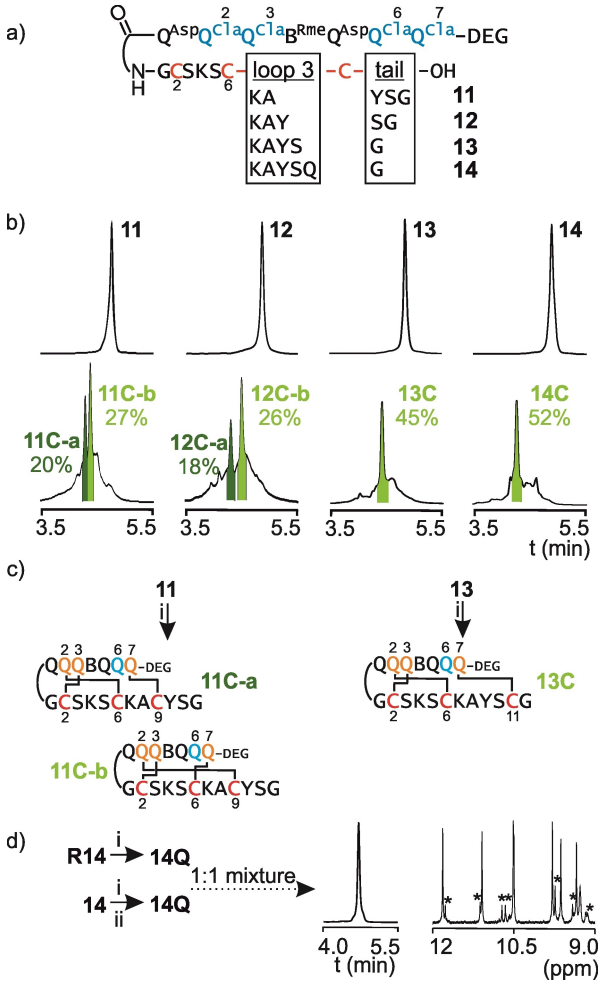

Figure 4. a) Foldamer-peptide hybrid sequences with four chloroacetamides and three Cys residues with variable loop3 sizes. b) HPLC chromatograms before and after cyclization. Percentages are yields calculated by peak integration and comparison with an internal standard. c) Cyclization trail of **11C** and **13C**. d) HPLC chromatogram and excerpt of the ^{1}H NMR spectrum (aromatic NH resonances) of a 1:1 mixture of **14Q** obtained from the cyclization of **R14** and of **14Q** obtained by quenching **14C**. Stars indicate signals belonging to an isomer of trimacrocycle **14Q.**

Cyclization of **11** and **12** showed two main products whose mass corresponded to a tricycle (Figure 4b). Due to their short loop3, we hypothesized that Cys9 (in **11**) and Cys10 (in **12**) reacted with $Q^{Cla}2$ in competition with Cys6, leaving the latter to react with $Q^{Cla}7$ (Figure 4c). In contrast, **13** and **14** yielded one main tricycle (Figure 4b). However, in comparison with the mono- and bicycle series, the chromatograms of **11C**–**14C** were less clean and isolated yields were lower. MS analysis revealed that all four starting materials contained impurities, despite showing one HPLC peak. To improve purity, subsequent sequences (precursors of tetracycles in the next section) were prepared via fragment condensation approach with the side chain protected Fmoc-foldamer-Gly-OH pre-synthesized on a Fmoc-Gly-SASRIN® resin and purified before condensation. In the case of **11**–**14**, accurate analysis of the reactions was hampered by the starting material impurities. Nevertheless, bicyclic products were detectable even after long incubation, suggesting that some "dead-ends" were met when reactions take a undesirable trail.

The progression of the macrocyclization of **14** was monitored by LC–MS in small time increments over 6 h (see Figure S17). Remarkably, a main monocycle and a main bicycle were observed to form successively, supporting the hypothesis that the smallest rings form faster and that Cys2, Cys6 and Cys12 residues react in this order. The reaction was overall slower than with bicycles. About 3 h were needed before chromatograms stopped evolving. After 6 h, cyclization reactions of **11**–**14** were quenched with benzyl mercaptan. Pure quenched trimacrocycles **11Q-a**, **11Q-b**, **12Q-a**, **13Q** and **14Q** could be isolated by preparative RP-HPLC and analyzed. Reference sequence **R14** was synthesized in which the foldamer and peptide were kept the same as in **14**, except for $Q^{Sbn}6$ which was already installed instead of $Q^{Cla}6$. **R14** was then cyclized, and the isolated product proved to be identical to **14Q**, proving that $Q^{Cla}6$ had not been involved, as anticipated (Figure 4d). This analysis also revealed that **14Q** contained about 8 % of another product (Figure 4d, ^{1}H NMR spectrum and S33). LC–MS did not indicate any obvious mass suggesting that another tricycle may have formed even with the longest loop3 and co-eluted with the main product.

Intrigued by the possible consequences of multi-macrocycle formation on the peptide conformation, we compared the CD spectra of linear **14** and cyclic **14Q**. Both spectra are dominated by CD bands belonging to the quinoline chromophores of the left-handed foldamer helix (Figure S49). A negative band near 390 nm and another near 260 nm were the most notable. Upon subtracting the CD spectra of **14** and **14Q**, a slight band remained near 260 nm, suggesting that the foldamer conformation is slightly different in the two compounds so that perfect subtraction of its contribution to the CD spectrum cannot be achieved. Another band was visible near 220 nm after subtraction, but it is not possible to tell whether it comes from variations in

the peptide contribution to the CD spectrum, or whether it also results from slight changes in the foldamer conformation since both the foldamer and the peptide absorb at 220 nm.

Tetracycle formation

To target $Q^{Cla}6$ in a fourth macrocycle, sequences **15–17** were designed (Figure 5a). They possess the same loop3 as **14** (-Lys-Ala-Tyr-Ser-Gln-), before Cys12, peptide loop4, and a fourth Cys residue. Because of the remote location of $Q^{Cla}6$ from Q7, a relatively long loop4 was designed with either six, eight, or ten AAs, bringing the fourth Cys residue to position 19, 21 or 23, respectively. Considering that Q^{Xxx} and B^{Rme} aromatic δ-amino acids are similar in size to a dipeptide, **15–17** are equivalent to 34-amino acid peptides. To enhance the overall purity of the resin-bound peptide fragment, a single coupling cycle was performed and coupling time was extended to 30 min at room temperature using a 10 equivalent excess of Fmoc-AA-OH with respect to the resin loading. Initial cyclizations in the bicarbonate buffer showed unexpectedly complex HPLC chromatograms. We suspected that folding and aggregation of the long peptides may be a source of complications. Indeed much sharper chromatograms were obtained upon performing reactions in the presence of chaotropic agents such as urea. Precursors **15–17** all yielded three tetracycles (e.g. **15C-a** to **15C-c**) distinguishable by LC–MS (Figures 5b, S21, S23, S25). Subsequent quenching with benzyl mercaptan resulted in a shift to higher retention times of most other chromatographic peaks (Figures 5b, quenched and S20, S22, S24), suggesting that they contained orphan Q^{Cla} units. MS analysis of the quenched products validated this hypothesis. The persistence of orphan Q^{Cla} units is a good indication that the helical template behaves as a rigid object even in the presence of the chaotropic agent: intramolecular reactions that require unfolding of the foldamer helix are disfavored. In the case of **15** and **16**, the three isomeric tetracycles could be isolated as pure or slightly cross-contaminated products (Figures S20, S22). Since all three isomers have the same molecular composition, their different retention times are noteworthy and suggest significant variations in their 3D arrangement, i.e. in the way they expose functionalities to the solvent and the stationary phase. This is a result of the peptide chain winding around the foldamer helix by different trails resulting in different cyclization patterns.

Cyclizations were monitored at small time increments by HPLC and LC–MS (Figures S20–S25). Figure 5c shows the example of **15**. The successive appearance of the mono-, bi- and tricycles before accumulation of the tetracycles was clearly evidenced. Given the outcome of tricyclization reactions (previous section), the Cys2/$Q^{Cla}3$, Cys6/$Q^{Cla}2$, Cys12/$Q^{Cla}7$, CysX/$Q^{Cla}6$ (X = 19, 21 or 23) reaction sequence was presumed to be favored, generating two sequence crossings of thioether bridges (Figure 5d, right). Models helped formulate hypotheses regarding the nature of the two other products. The allowed and forbidden reactions (because the peptide is too short to reach a certain Q^{Cla} unit) were systematically examined (Figure S46). For example, if another Cys residue than Cys2 reacts with $Q^{Cla}3$, Cys2 necessarily remains an orphan site. After the first Cys2/$Q^{Cla}3$ reaction, Cys6 may react with $Q^{Cla}7$ instead of $Q^{Cla}2$ (Figure 5d, right). This pattern was not detected for compounds **9** and **10**, but appeared for **11–14** and appears to be more significant with **15–17**. It thus seems that the ability of Cys6 to quickly reach $Q^{Cla}2$ decreases upon elongating the peptide beyond Cys6, although the additional AAs are not involved in the loop. If Cys6 reacts with $Q^{Cla}7$, Cys12 can only react with $Q^{Cla}2$ as the remaining $Q^{Cla}6$ is out of reach. The last remaining Cys21 then reacts with the remaining $Q^{Cla}6$. A third plausible tetracycle may form after the Cys2/$Q^{Cla}3$, Cys6/$Q^{Cla}2$ reactions when Cys21 reacts with $Q^{Cla}7$ before Cys12 does, leaving $Q^{Cla}6$ as the only option for Cys12 even though this pathway is not a priori favored (Figure 5d, middle). In summary, only three tetracycles form out of 24 formal possibilities, and one of the three is favored over the other two. Figure 5e shows the structural formula of the presumably dominant form of **15C** and provides a visual measure on the large macrocycles that spontaneously form based on structural preferences.

Recapitulation of a more selective trail via $Q^{Cla}1$

We then assessed a second cyclization trail via $Q^{Cla}1$ instead of $Q^{Cla}7$. This choice was again guided by reasonable predictions based on the relative distances between foldamer units and the assumption that smaller cycles form faster. We first verified that the Cys2/$Q^{Cla}3$ plus Cys6/$Q^{Cla}2$ (or Cys7/$Q^{Cla}2$) reaction sequence could be performed selectively in presence of $Q^{Cla}1$. Compounds **18** and **19** which possess two Cys residues and three Q^{Cla} units were synthesized for this purpose (Figure 6a). After 3 h of reaction in a bicarbonate buffer, a major bicyclic product was observed in both cases (**18C** and **19C** in Figures 6b, S26, S29). The unreacted chloroacetamide was quenched with benzyl mercaptan to yield **18Q** and **19Q**, respectively. Separately, reference macrocycle **R18** was synthesized with the same peptide as **18** and a $Q^{Sbn}1$-$Q^{Cla}2$-$Q^{Cla}3$ segment, that is, with a benzyl thioether already installed on Q1. The cyclization of **R18** yields a product analytically identical to **18Q** (Figures 6d, S28), indicating that $Q^{Cla}1$ had remained free in **18C** (Figure 6c, left).

Finally, a tetracycle was targeted from precursor **20** (Figure 6a). This sequence comprises the same peptide segment as **15** with Cys residues in 2, 6, 12 and 19, as well as four chloroacetamides at Q1, Q2, Q3 and at the N-terminus. Cyclization in the presence of urea was monitored by LC–MS (Figure S31). The chromatogram did not evolve after 24 h and the reaction was stopped after 48 h. One major tetracycle was detected and isolated (Figure 6b, right). Its NMR spectrum demonstrates that it is a unique well-defined product (see Supporting Information section 3). A second, minor, tetracyclic product was not isolated (star in Figure 6b). A slightly broadened HPLC peak corresponding to a tricycle dead end was also observed. Further analysis (e.g.

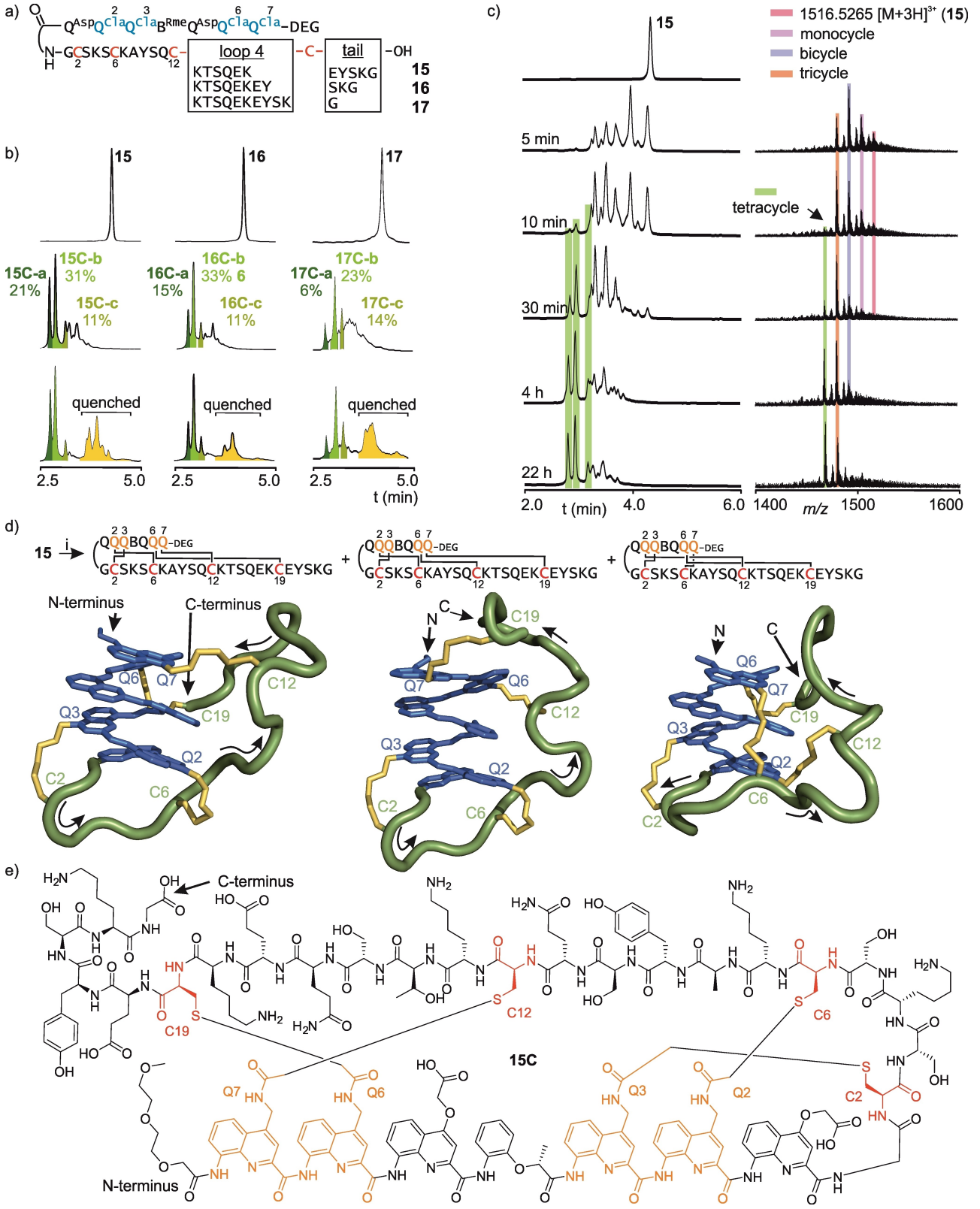

Figure 5. a) Foldamer-peptide hybrid sequences with four chloroacetamides and four Cys residues with variable loop4 sizes. b) From top to bottom: HPLC chromatograms before cyclization, after cyclization and after quenching with benzyl mercaptan. Tetracycles are marked with different green colors. Quenched sequences are marked with yellow. Percentages are yields calculated by peak integration and comparison with an internal standard. c) Parallel HPLC and ESI-MS monitoring of the cyclization of **15**. MS spectra correspond to the mass spectrum acquisition for the time segment 2.5–5.0 min of the chromatogram. HPLC peaks of tetracyclic products are marked in green. d) Plausible structures of three **15C** products. The foldamer is represented in blue, the peptide main chain is schematized as a green tube, and thioether-containing linkages are shown in yellow. Arrows indicate N- to C-terminus orientation. e) Structural formula of **15C**.

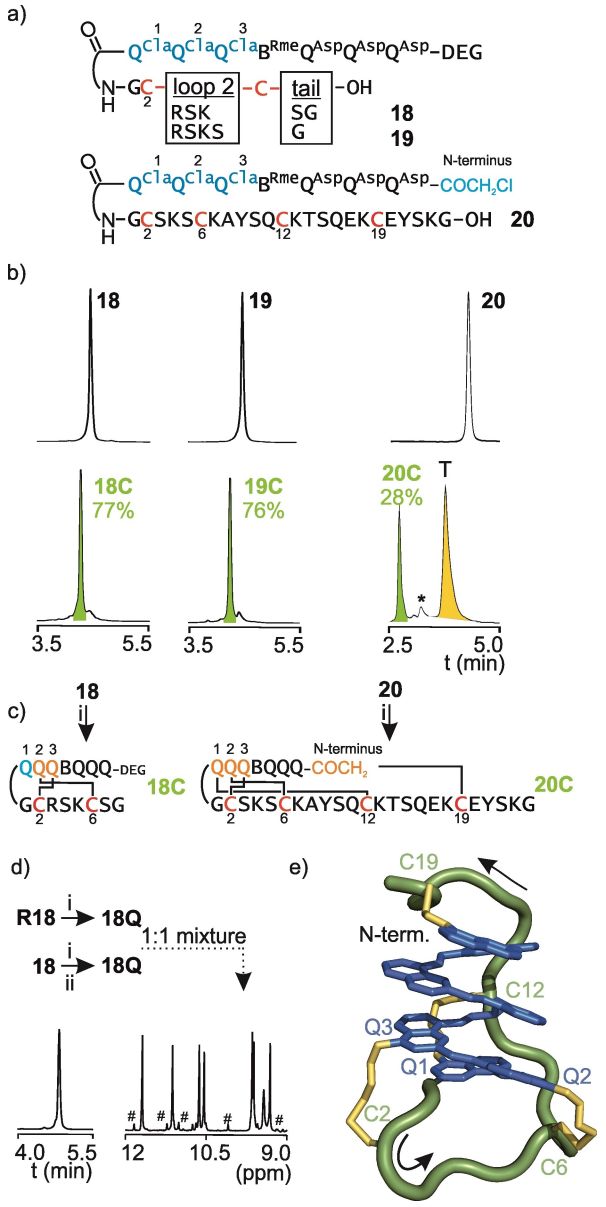

Figure 6. a) Foldamer-peptide hybrid sequences with chloroacetamides on Q1 b) HPLC chromatograms before (top) and after cyclization (bottom). Bicycles **18C**, bicycle **19C** and tetracycle **20C** are marked in green. Remaining dead-end tricycles (T) are marked in orange. The star indicates a second minor tetracycle. Percentages are yields calculated by peak integration and comparison with an internal standard. c) Preferred cyclization trails of **18** and **20**. d) HPLC chromatogram and excerpt of the ^{1}H NMR spectrum (aromatic NH resonances) of a 1:1 mixture of **18Q** obtained from the cyclization of either **R18** or by quenching **18C**. # indicate signals belonging to an impurity. e) Plausible structure of **20C**. The foldamer is colored in blue, the peptide main chain is schematized as a green tube, and thioether-containing linkages are shown in yellow. Arrows indicate N- to C-terminus orientation. The C-terminal EYSKG segment is omitted for clarity.

isolation and NMR spectroscopy) was not performed to determine whether this peak corresponds to one product to several products of identical mass. Given the demonstrated Cys2/Q^{Cla}3 and Cys6/Q^{Cla}2 selectivity, and the fact that Cys12 can hardly reach the N-terminal chloroacetamide, the connectivity shown in Figures 6c and 6e with three sequence crossings can be reasonably proposed for **20C**. The chromatographic behavior of these compounds confirms a trend noted in earlier experiments: when comparing the retention time of a given acyclic precursor to that of the products that form successively (first monocycles, then bicycles, then tricyles, etc.), one notes that migration on the reverse-phase faster the further the macrocyclization is advanced, as if stitching the peptide progressively shields the hydrophobic aromatic foldamer helix from exposure to water.

Conclusion

The concept of reaction trails has been introduced where a peptide can selectively covalently link itself at up to four sites of a structurally defined rigid helical aromatic foldamer scaffold. Selective differential multimacrocyclization proceeds with good efficiency despite similar reaction partners being involved at each step, which in principle would allow for the formation of numerous isomeric products. The most outstanding feature of the multicyclic products is that the macrocycles produced are different in size and geometry: both the peptide and aromatic foldamer segments contained in each macrocycle of a given multicyclic product differ. The efficiency of the process rests on the fact that shorter cycles form faster, and on the structural stability of the scaffold. The trails can be to a large extent predicted and designed. By comparison with shape persistent macrocycles[19] and multicycles[20] whose formation is often favored by the preorganization of the non-cyclic precursor, the macrocycles formed here may be coined semi-shape persistent: only part of their non-cyclic precursor is structurally defined, yet this is sufficient to promote selective cyclization.

Multiple directions for further development can be envisaged from this point including, but not limited to, challenging shorter loops, introducing repeat cyclic motifs (constant peptide loop size and constant number of units between reactive quinoline side chains), or investigating the dependence on stereochemistry. Regarding this latter aspect, using a *P* foldamer helix instead of an *M* helix to cyclize L-peptides amounts to cyclizing D-peptides on the *M*-helix, that is, to offer the same loop size and trail, but with the possibility to improve or worsen selectivity because the relative stereochemistry of the peptide and helix is different. Other lines of development include using the macromulticycles for multivalent protein recognition and, eventually, their incorporation in display selection experiments. Progress along these lines will be reported in due course.

Acknowledgements

We thank the Deutsche Forschungsgemeinschaft (DFG) for financial support via project HU1766/2-1 and CRC1309-C7 (project ID 325871075). We thank Daniel Gill and Binhao Teng for contributing some building block precursors as well as Lars Allmendinger for assistance with NMR measure-

ments. Open Access funding enabled and organized by Projekt DEAL.

Conflict of Interest

The authors declare no conflict of interest.

Data Availability Statement

The data that support the findings of this study are available from the corresponding author upon reasonable request.

Keywords: Aromatic Foldamer · Helical Conformation · Macrocycle · Peptide · Reaction Trail

[1] a) V. Martí-Centelles, M. D. Pandey, M. I. Burguete, S. V. Luis, *Chem. Rev.* **2015**, *115*, 8736–8834.
[2] S. Ma, *in Handbook of Cyclization Reactions*, Wiley-VCH, Weinheim, **2010**.
[3] a) A. A. Vinogradov, Y. Yin, H. Suga, *J. Am. Chem. Soc.* **2019**, *141*, 4167–4181; b) W. Liu, S. J. de Veer, Y.-H. Huang, T. Sengoku, C. Okada, K. Ogata, C. N. Zdenek, B. G. Fry, J. E. Swedberg, T. Passioura, D. J. Craik, H. Suga, *J. Am. Chem. Soc.* **2021**, *143*, 18481–18489.
[4] For selected reviews: a) C. J. White, A. K. Yudin, *Nat. Chem.* **2011**, *3*, 509–524; b) L. Reguera, D. G. Rivera, *Chem. Rev.* **2019**, *119*, 9836–9860; c) Y. H. Lau, P. de Andrade, Y. Wu, D. R. Spring, *Chem. Soc. Rev.* **2015**, *44*, 91–102; d) C. Bechtler, C. Lamers, *RSC Med. Chem.* **2021**, *12*, 1325–1351.
[5] a) T. R. Oppewal, I. D. Jansen, J. Hekelaar, C. Mayer, *J. Am. Chem. Soc.* **2022**, *144*, 3644–3652; b) Y. Wu, H. F. Chau, W. Thor, K. H. Y. Chan, X. Ma, W. L. Chan, N. J. Long, K. L. Wong, *Angew. Chem. Int. Ed.* **2021**, *60*, 20301–20307; *Angew. Chem.* **2021**, *133*, 20463–20469; c) J. E. Montgomery, J. A. Donnelly, S. W. Fanning, T. E. Speltz, X. Shangguan, J. S. Coukos, G. L. Greene, R. E. Moellering, *J. Am. Chem. Soc.* **2019**, *141*, 16374–16381; d) Y. H. Lau, Y. Wu, M. Rossmann, B. X. Tan, P. De Andrade, Y. S. Tan, C. Verma, G. J. Mckenzie, A. R. Venkitaraman, M. Hyvönen, D. R. Spring, *Angew. Chem. Int. Ed.* **2015**, *54*, 15410–15413; *Angew. Chem.* **2015**, *127*, 15630–15633; e) J. Ceballos, E. Grinhagena, G. Sangouard, C. Heinis, J. Waser, *Angew. Chem. Int. Ed.* **2021**, *60*, 9022–9031; *Angew. Chem.* **2021**, *133*, 9104–9113; f) M. S. Islam, S. L. Junod, S. Zhang, Z. Y. Buuh, Y. Guan, M. Zhao, K. H. Kaneria, P. Kafley, C. Cohen, R. Maloney, Z. Lyu, V. A. Voelz, W. Yang, R. E. Wang, *Nat. Commun.* **2022**, *13*, 350.
[6] a) T. Katoh, T. Sengoku, K. Hirata, K. Ogata, H. Suga, *Nat. Chem.* **2020**, *12*, 1081–1088; b) S. Imanishi, T. Katoh, Y. Yin, M. Yamada, M. Kawai, H. Suga, *J. Am. Chem. Soc.* **2021**, *143*, 5680–5684; c) C. W. Lin, M. J. Harner, A. E. Douglas, V. Lafont, F. Yu, V. G. Lee, M. A. Poss, J. F. Swain, M. Wright, D. Lipovšek, *Angew. Chem. Int. Ed.* **2021**, *60*, 22640–22645; *Angew. Chem.* **2021**, *133*, 22822–22827.
[7] a) X. Hou, Z. Wang, J. Lee, E. Wysocki, C. Oian, J. Schlak, Q. R. Chu, *Chem. Commun.* **2014**, *50*, 1218–1220; b) Y. C. Teo, H. W. H. Lai, Y. Xia, *Chem. Eur. J.* **2017**, *23*, 14101–14112; c) J. F. Reuther, J. L. Dees, I. V. Kolesnichenko, E. T. Hernandez, D. V. Ukraintsev, R. Guduru, M. Whiteley, E. V. Anslyn, *Nat. Chem.* **2018**, *10*, 45–50.
[8] K. C. Nicolaou, J. S. Chen, *Chem. Soc. Rev.* **2009**, *38*, 2993–3009.
[9] a) S. Chen, D. Bertoldo, A. Angelini, F. Pojer, C. Heinis, *Angew. Chem. Int. Ed.* **2014**, *53*, 1602–1606; *Angew. Chem.* **2014**, *126*, 1628–1632; b) W. Liu, Y. Zheng, X. Kong, C. Heinis, Y. Zhao, C. Wu, *Angew. Chem. Int. Ed.* **2017**, *56*, 4458–4463; *Angew. Chem.* **2017**, *129*, 4529–4534; c) G. J. J. Richelle, S. Ori, H. Hiemstra, J. H. Van Maarseveen, P. Timmerman, *Angew. Chem. Int. Ed.* **2018**, *57*, 501–505; *Angew. Chem.* **2018**, *130*, 510–514.
[10] a) C. Wu, J.-C. Leroux, M. A. Gauthier, *Nat. Chem.* **2012**, *4*, 1044–1049; b) H. Dong, J. Li, H. Liu, S. Lu, J. Wu, Y. Zhang, Y. Yin, Y. Zhao, C. Wu, *J. Am. Chem. Soc.* **2022**, *144*, 5116–5125.
[11] P. J. Robinson, N. J. Bulleid, *Cells* **2020**, *9*, 1994.
[12] Reaction trail describes the sequence of reactions needed to produce a desired product which is opposed to reaction pathway, which describes the successive steps at the molecular level which take place in a chemical reaction.
[13] S. Dengler, P. K. Mandal, L. Allmendinger, C. Douat, I. Huc, *Chem. Sci.* **2021**, *12*, 11004–11012.
[14] a) J. M. Rogers, S. Kwon, S. J. Dawson, P. K. Mandal, H. Suga, I. Huc, *Nat. Chem.* **2018**, *10*, 405–412; b) C. Tsiamantas, S. Kwon, C. Douat, I. Huc, H. Suga, *Chem. Commun.* **2019**, *55*, 7366–7369; c) C. Tsiamantas, S. Kwon, J. M. Rogers, C. Douat, I. Huc, H. Suga, *Angew. Chem. Int. Ed.* **2020**, *59*, 4860–4864; *Angew. Chem.* **2020**, *132*, 4890–4894.
[15] a) B. Baptiste, C. Douat-Casassus, K. Laxmi-Reddy, F. Godde, I. Huc, *J. Org. Chem.* **2010**, *75*, 7175–7185; b) D. Bindl, P. K. Mandal, I. Huc, *Chem. Eur. J.* **2022**, *28*, e202200538; c) S. J. Dawson, Á. Mészáros, L. Pethő, C. Colombo, M. Csékei, A. Kotschy, I. Huc, *Eur. J. Org. Chem.* **2014**, 4265–4275; d) T. Qi, V. Maurizot, H. Noguchi, T. Charoenraks, B. Kauffmann, M. Takafuji, H. Ihara, I. Huc, *Chem. Commun.* **2012**, *48*, 6337–6339.
[16] D. Bindl, E. Heinemann, P. K. Mandal, I. Huc, *Chem. Commun.* **2021**, *57*, 5662–5665.
[17] X. Hu, S. J. Dawson, Y. Nagaoka, A. Tanatani, I. Huc, *J. Org. Chem.* **2016**, *81*, 1137–1150.
[18] Initial experiments were carried out at pH 10 in TEA buffer. It was observed, that the ε-amine of Lys residues can act as nucleophiles at that pH. Switching to pH 8.5 prevented the side reaction.
[19] W. Zhang, J. S. Moore, *Angew. Chem. Int. Ed.* **2006**, *45*, 4416–4439; *Angew. Chem.* **2006**, *118*, 4524–4548.
[20] J. Lin, J. Wu, X. Jiang, Z. Li, *Chin. J. Chem.* **2009**, *27*, 117–122.

Manuscript received: July 28, 2022
Accepted manuscript online: August 22, 2022
Version of record online: September 29, 2022